Computers and Fluids 314 (2026) 107085

Contents lists available at ScienceDirect

Computers and Fluids

journal homepage: www.elsevier.com/locate/compfluid

Dresden6—Current status and future of morphology-adaptive Eulerian modeling of multiphase flows

Fabian Schlegel [a,*], Amine Ben Hadj Ali [i], Marco Colombo [b], Edo Frederix [d], Victor Habiyaremye [d], Susann Hänsch [a], Thomas Höhne [a], Benjamin Krull [a], Ronald Lehnigk [a], Dirk Lucas [a], Richard Meller [a], Mohit P. Tandon [h], Michele Cristina Pedroso [f,g], Juho Peltola [c], Matej Tekavčič [e]

[a] Helmholtz-Zentrum Dresden-Rossendorf e.V., Bautzner Landstr. 400, 01328 Dresden, Germany
[b] School of Mechanical, Aerospace and Civil Engineering, University of Sheffield, Sheffield S1 4TD, United Kingdom
[c] VTT Technical Research Center Ltd., Tekniikantie 21, 02150 Espoo, Finland
[d] NRG PALLAS, Westerduinweg 3, 1755 LE Petten, The Netherlands
[e] Reactor Engineering Division, Jožef Stefan Institute, Jamova cesta 39, 1000 Ljubljana, Slovenia
[f] Federal University of Santa Catarina, Mechanical Engineering Faculty, 88035-972, Florianópolis, Brazil
[g] Petrobras Research Center, 21941-915, Rio de Janeiro, Brazil
[h] Siemens Industry Software, Gurgaon, India
[i] Ansys Germany GmbH, Industriestr. 2, 70565 Stuttgart, Germany

ARTICLE INFO

Keywords:
Numerical simulation
Multiphase flows
Morphology-adaptive method
Separated effect tests
Integral tests

ABSTRACT

Multiphase flows are of great relevance to a wide range of industries, and their simulation using Computational Fluid Dynamics (CFD) is an important pillar for conducting design studies and gaining physical insight. However, a particular challenge in the simulation of multiphase flows is the occurrence of different morphologies or flow regimes, i.e. dispersed vs. segregated. The established simulation frameworks that have been developed over the years are usually only applicable to a specific morphology and level of detail. The simulation of a combination of morphologies is particularly challenging, and adaptive approaches are sought where the trade-off between level of detail and time to solution is mainly a matter of spatial resolution, rather than the fundamental choice of a method. In this respect, the Euler-Euler model has crucial properties that make it a good basis. This paper gives an overview of existing morphology-adaptive Eulerian methods, also often referred to as hybrid Eulerian methods. It is the result of a joint effort of the Dresden6 initiative, a loose association of research groups already active in this field. It gives an honest picture of current shortcomings and future development prospects. The aim of the work is to start a homogenization process by establishing a common terminology and listing suitable test cases that can be used for benchmarking, i.e. verification and validation.

1. Introduction

Multiphase flows play a central role in many industrial sectors, e.g., nuclear engineering, chemical and process engineering, the automotive industry, and the energy industry. The optimization of many processes in terms of energy and resource efficiency requires detailed knowledge about the underlying, complex physics. Numerical simulations are a promising way to gain insights into multiphase flows, which are not always accessible by experiments, for example due to a lack of suitable measurement techniques, extreme conditions (e.g., high pressures and temperatures), lack of optical accessibility or high costs. Shorter development cycles in many industrial sectors increase the need for process digitalization, e.g., by performing virtual validation and developing digital twins for earlier detection of safety or efficiency problems. Numerical simulations can significantly contribute here if they fulfill certain requirements. These are, among others, a short time-to-solution, robustness of the underlying algorithms, usability, documentation on theory and application, flexibility, and applicability for complex geometries.

Many examples of the complexity of multiphase flows can be found in the chemical and process engineering industry, which has to undergo a transformation towards net-zero carbon dioxide emissions. This requires the conversion and optimization of existing technologies,

* Corresponding author.
E-mail address: f.schlegel@hzdr.de (F. Schlegel).

https://doi.org/10.1016/j.compfluid.2026.107085
Received 30 September 2025; Received in revised form 30 March 2026; Accepted 13 April 2026
Available online 17 April 2026

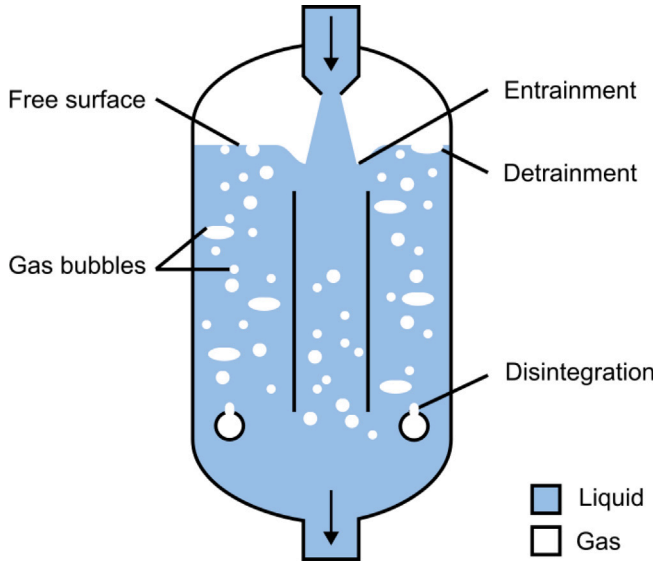

Fig. 1. Sketch of a jet-loop reactor with occurring mechanisms for multiphase flows.

and also the development of new processes, e.g., a closed material cycle to produce plastics. The majority of those processes involve gas–liquid two-phase flows. The processes are typically developed on a small scale in laboratories and scaled up with costly pilot plant test campaigns. The optimization requires many expensive trials, where numerical simulation can serve as a cost-efficient alternative. An example of a modern jet-loop reactor is shown in Fig. 1. The sketch shows a global co-existence of various *two-phase flow morphologies* in the system, i.e., small (gas bubbles) and large scale (free surface) two-phase structures present in the flow. Moreover, during operation these two-phase flow morphologies can transform into each other across the free surface via entrainment and detrainment, or by bubble disintegration processes.

Reliable predictions of two-phase flows with co-existing morphologies also play a crucial role in the safety analysis of nuclear reactors. A representative example is the scenario of a pressurized thermal shock, which may occur during the emergency cooling of a nuclear reactor, shown schematically in Fig. 2. It is evident that almost all morphologies and transfers between them are present.

In particular the huge range of scales and the different flow regimes that can appear even in a very simple geometry like a pipe (segregated, bubbly, annular, or slug flow) remain a challenging task. The level of complexity increases further if counter-current flows or wave breaking phenomena are of interest. Over the last decades several numerical methods have been developed to simulate the behavior of interfaces between moving fluids [1–3]. We will categorize the methods into deterministic and stochastic methods, based on the predictability of the location of the interface between the physical phases (Fig. 3). We will call a method deterministic if the interface location and shape is predicted without any uncertainty by the simulation method. Contrary, we will call a method stochastic, if the prediction of the interface is only a probability distribution function, and, hence, multiple realizations with different probabilities are possible. Stochastic methods are well suited for small-scale interfaces (dispersed flows, unresolved morphology), and deterministic methods are well suited for large-scale interfaces (resolved morphology). For the latter several methods have been developed, all having their advantages and disadvantages, e.g., Lagrangian methods, namely marker and cell or front-tracking methods [4], or Eulerian methods, namely (conservative) level-set [5], phase-field [6,7] or geometric/algebraic volume-of-fluid [VOF, 8,9]. Deterministic modeling reaches its limits as soon as there is a prohibitively large number of small-scale structures, i.e. fluid or solid particles. For dispersed flow morphologies, stochastic methods are also well developed, e.g., Euler–Lagrange, representing the small-scale interfaces as groups of spheres, or the Euler-Euler model, utilizing averaging, resulting in the idea of interpenetrating continua [10]. It should be noted that Euler–Lagrange can be considered a deterministic method as long as there are no statistical quantities present in the equations of motion. However, unsteady and intermittent features of some flow regimes that possess some degree of determinism, e.g., slug and plug flows in pipes, are difficult to capture with stochastic methods, due to the averaging procedure involved. Despite the huge progress in the development of numerical methods for multiphase flows, the simulation of a flow where the morphology is not known a priori, and which involves the co-existence of both unresolved (dispersed) and resolved (large-scale) morphologies lacks a robust morphology-adaptive or hybrid framework.

It is clear that such a framework is mainly needed for industrial scale applications, where the mesh resolution due to limited computing resources does not allow high-fidelity simulations. However, with increasing computing power it is possible to resolve interfaces locally, where grid resolution is sufficient. Hence, such a numerical framework will need the capability to apply locally different modeling strategies depending on the flow morphology. To achieve this, appropriate morphology transfer models have to be implemented, which require a sub-model or criteria to detect the transition of the flow regime.

What are the demands for the successful and sustainable application of morphology-adaptive methods in industrial applications? First of all, a well verified and validated simulation framework is required, producing results in a reliable and robust manner. The results have to be accompanied by an uncertainty analysis, to check the sensitivity against errors. To obtain a wider acceptance of morphology-adaptive methods, homogenization of the models is a key prerequisite, which means that simulation results have to be comparable between the different simulation frameworks. This requires a common understanding of the theory of the methods and a commonly accepted terminology. Furthermore, a well-defined verification and validation database is needed, which covers the important physical phenomena and allows for cross-checking between the different simulation frameworks. The ultimate goal would be to enable morphology-adaptive methods to become part of a regulatory process (licensing), like nuclear system codes [12]. Those system codes have been thoroughly validated during the last three decades and the process yielded a homogenization of various, separately developed codes world-wide. Within the homogenization process a database of *separated effect tests* and *integral tests* has been developed.

To start such a homogenization process specifically for **morphology-adaptive Eulerian methods** is the aim of this paper and the *Dresden6* initiative, founded in 2023 at the Multiphase Flow Conference in Dresden at Helmholtz-Zentrum Dresden-Rossendorf e.V. The name of the initiative goes back to the six founding research organizations, namely

- Jožef Stefan Institute, Slovenia,
- Nuclear Research and Consultancy Group, the Netherlands,
- VTT Technical Research Center Ltd., Finland,
- Helmholtz-Zentrum Dresden-Rossendorf e.V., Germany,
- University of Sheffield, United Kingdom, and
- Federal University of Santa Catarina, Brazil.

In the meantime two more organizations, namely Ansys Germany and Siemens Industry Software, have joined the initiative. The members share the common goal of developing a theoretical background for morphology-adaptive Eulerian methods. The definition of commonly accepted separate effect and integral tests should allow for comparison between the different methodologies developed in the research groups. Furthermore, the initiative aims for identification of missing phenomena, which have not yet been covered by the developed

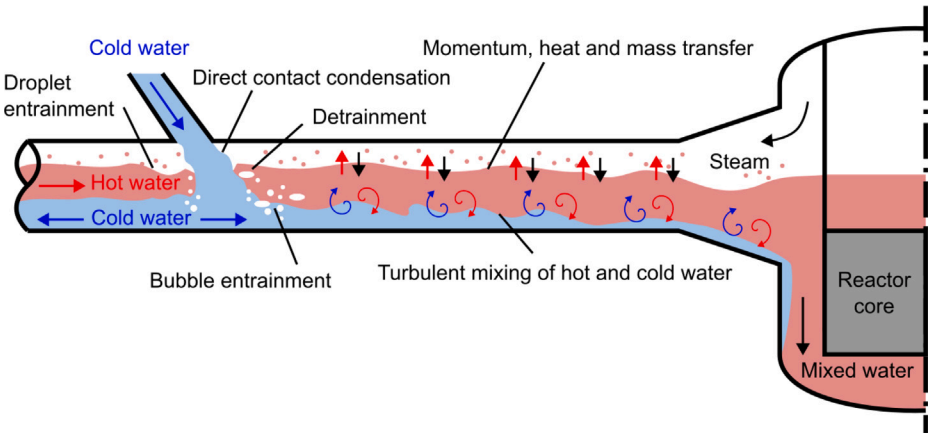

Fig. 2. Sketch of a pressurized thermal shock scenario for emergency cooling in nuclear reactor safety analysis.

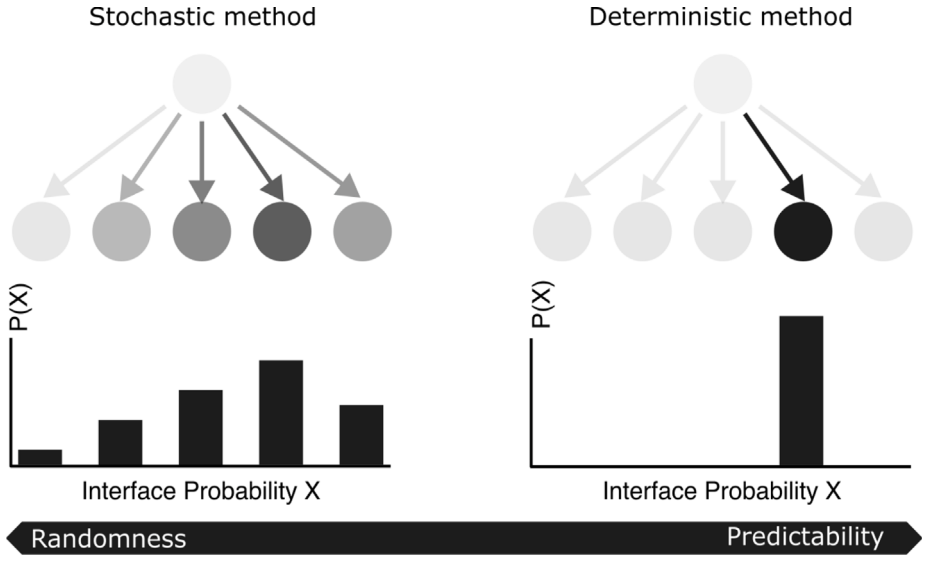

Fig. 3. Concept of stochastic and deterministic methods with respect to the prediction of the interface between two liquids.
Source: The image is adopted from [11].

morphology-adaptive Eulerian methods, and allows for a long-term planning and work-share between the members.

This paper will make a first attempt to define a common theoretical basis and terminology for morphology-adaptive Eulerian methods in Section 2, including the discussion of the compatibility of stochastic and deterministic methods, and some thoughts on turbulence modeling. In Section 3 we will introduce the morphology-adaptive Eulerian methods of the different research groups in Dresden6. Section 4 will define and describe a set of separated effect and integral tests. Finally, the paper will present some future challenges yet to be overcome, in Section 5.

2. Theoretical concept of morphology-adaptive Eulerian methods

Several research groups are active in the development of morphology-adaptive Eulerian methods. The developed methods and implementations are quite similar, but also differ in some aspects. To increase the acceptance of morphology-adaptive Eulerian methods, and to allow for joint efforts and knowledge transfer, a common terminology and a common understanding of the fundamental equations is needed. Hence, Section 2.1 presents the terminology on which the Dresden6 group has agreed and the fundamental equations in Section 2.2. Furthermore, possible turbulence modeling strategies are discussed in Section 2.3 and some remarks on accuracy and performance will be given in Section 2.4.

2.1. Terminology

As already stated in the introduction, a key aspect of any homogenization process is a common terminology to describe the method and the used models and processes therein. A widely accepted terminology to describe multiphase flows can be obtained from physics, e.g., when looking at flow regimes terms like ‘dispersed’, ‘segregated’ and ‘large-scale’ interfaces, which are well-defined. However, when looking at morphology-adaptive Eulerian methods things become less clear and involve physical as well as numerical considerations. A generic overview of the basic idea of a morphology-adaptive Eulerian method is given in Fig. 4. In the following we will present a comprehensive terminology, extensively discussed between the authors, to describe the morphologies and transfer processes from a numerical point of view. An overview is shown in Fig. 5.

A **physical phase** defines a region of space, constituted by the same substance and in the same physical state, e.g., gas, liquid, or solid. Note, if only the term ‘phase’ is used without any attribute, this always refers to a physical phase. Each physical phase may come with multiple morphologies. Contrary to a physical phase, a **numerical phase** represents a numerical concept. Each numerical phase introduces a set of conservation equations, e.g., mass, momentum and energy. A numerical phase can either represent all morphologies of a physical phase, or

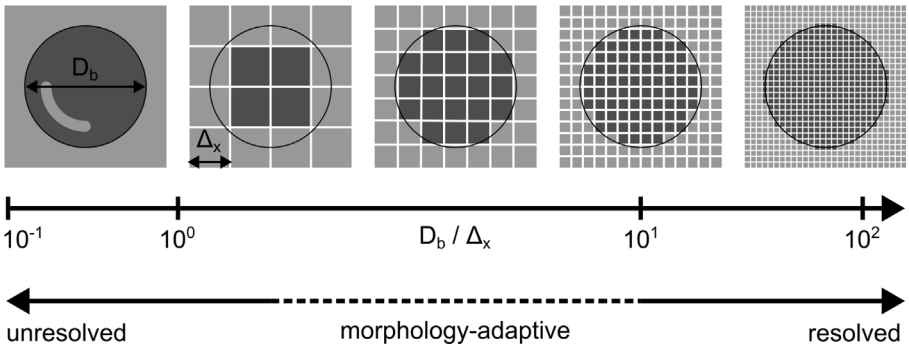

Fig. 4. Sketch of the numerical morphologies in multiphase flow simulations with respect to the spatial resolution that has to be considered when developing a morphology-adaptive Eulerian method.

a separate numerical phase can be defined for each morphology of a physical phase.

A **morphology** defines the shape of a two-phase structure that occurs with a characteristic size (scale), e.g., a bubble, a droplet, a thin-film or a stratified interface, in a multiphase flow. As such, it always involves an interface between two physical phases. Depending on resolution requirements, e.g. on the spatial resolution of the computational grid, we can further distinguish these into **numerical morphologies**. A numerical morphology is considered as **resolved morphology**, if the discretization captures all of its relevant features. For the Euler-Euler model a filter, i.e., averaging operator, is typically applied to the conservation equations, either explicitly or implicitly by the choice of grid cell size and time step size. In case their characteristic length and time scales are larger than the filter width, a numerical morphology is considered as explicitly resolved and will be represented in a deterministic manner. On the other hand, a numerical morphology is considered as **unresolved morphology**, if the discretization does not capture all of its relevant features. If the characteristic length and time scales are smaller than the filter width additional closure terms are required for the conservation equations. The numerical morphology will be modeled in what we call stochastic modeling. In-between resides the **partially-resolved morphology** for a discretization that only captures a sub-set of the relevant features of a numerical morphology, i.e., if the characteristic length and time scales are in the same order as the filter width. This typically appears in a region where transfer between a stochastic and the deterministic representation takes place, but is not limited to it. In the following we use morphology, but refer to numerical morphology.

The behavior of a multiphase flow, including its morphology, can be predicted with numerical simulations by solving a set of partial differential equations. A **morphology-adaptive Eulerian method**, or also referred to as hybrid Eulerian method, is based on the theory of interpenetrating continua that considers all morphologies of a physical phase and allows them to co-exist. Depending on the local discretization, the method dynamically switches between a stochastic and a deterministic representation of a morphology. Based on how the morphologies are distinguished in the numerical representation of the physical phase, two sub-classes can be defined. Within a **blended method** the distinction between resolved, partially-resolved and unresolved morphologies is made based on a blending method, which is computed based on the local flow conditions. The number of numerical phases is independent from the number of possible morphologies and equal to the number of physical phases. Such methods are also referred to as single-field methods. As an alternative, each physical phase can be decomposed into multiple numerical phases according to the existing morphologies. This will result in the **separated method** subclass. Here, the number of numerical phases depends on the number of possible morphologies. The distinction between resolved, partially-resolved and unresolved morphologies is made via the local existence of the corresponding numerical phase. Such methods are also referred to as multi-field methods.

Between the numerical phases, **transfers** have to be defined to represent any exchange of a conserved quantity, e.g., mass, momentum and/or energy between numerical phases. A transfer can be categorized according to Fig. 5 into **phase transfer**, **morphology transfer**, and **phase-morphology transfer**. Examples for phase transfer are direct contact condensation or film boiling processes. For the separated method a sub-category of phase transfer named resolution-adaptive transfer is required. It accounts for a local change in the morphology of a physical phase numerically, if a structure moves into a region of higher resolution, or physically, if a structure grows/shrinks, e.g., due to coalescence or breakup. The resolution-adaptive transfer models implicitly include a mesh dependence. Entrainment of gas or liquid, bubble bursting, deposition of droplets, break-up and coalescence of bubbles are typical examples for empirical morphology transfers. The well-known interfacial closures for momentum exchange in the Euler-Euler model (e.g., among others, drag, lift, turbulent dispersion, virtual mass, and wall lubrication) are part of the category phase-morphology transfers, which might also include phenomena like nucleate boiling.

2.2. Basic equations

The concept of interpenetrating continua for numerical simulation of multiphase flows has been intensively discussed in literature, e.g., by Drew and Passman [13], Ishii and Hibiki [10], Prosperetti and Tryggvason [14] and Yeoh and Tu [15] to name a few. There is no unique naming convention for this approach, it is frequently referred to as the Euler-Euler model, but multi-fluid model, two-fluid model, or Eulerian multi-fluid model are also common names. Note that the term two-fluid refers to the idea of interpenetrating continua and does not limit the model to two fluids. The derivation of the phase-averaged Navier–Stokes equations in literature mainly differs in terms of the underlying averaging method, i.e., authors use ensemble-, time- or volume-averaging. The final equations look the same, but the choice of the averaging method influences the formulation of interfacial closure models and the interpretation of results. According to Drew and Passman [13], it is possible to obtain from one realization of a statistically stationary macroscopic process an infinite number of other realizations by shifting the time origin by an arbitrary period. Such a process is named an *ergodic* process, and allows to equally perform ensemble and time averaging. In the following we will use ensemble averaging and follow mainly the derivation of Drew and Passman [13].

The ensemble average for the observable f is defined as

$$\langle f \rangle(\mathbf{x}, t) = \int_{\epsilon} f(\mathbf{x}, t, \gamma) dm(\gamma) \tag{1}$$

where $\mathbf{x}$ represents a spatial coordinate, t the time, and $dm(\gamma)$ the probability of occurrence of realization γ within the collection of macroscopically identical systems (ensemble), referred to as ϵ. Further,

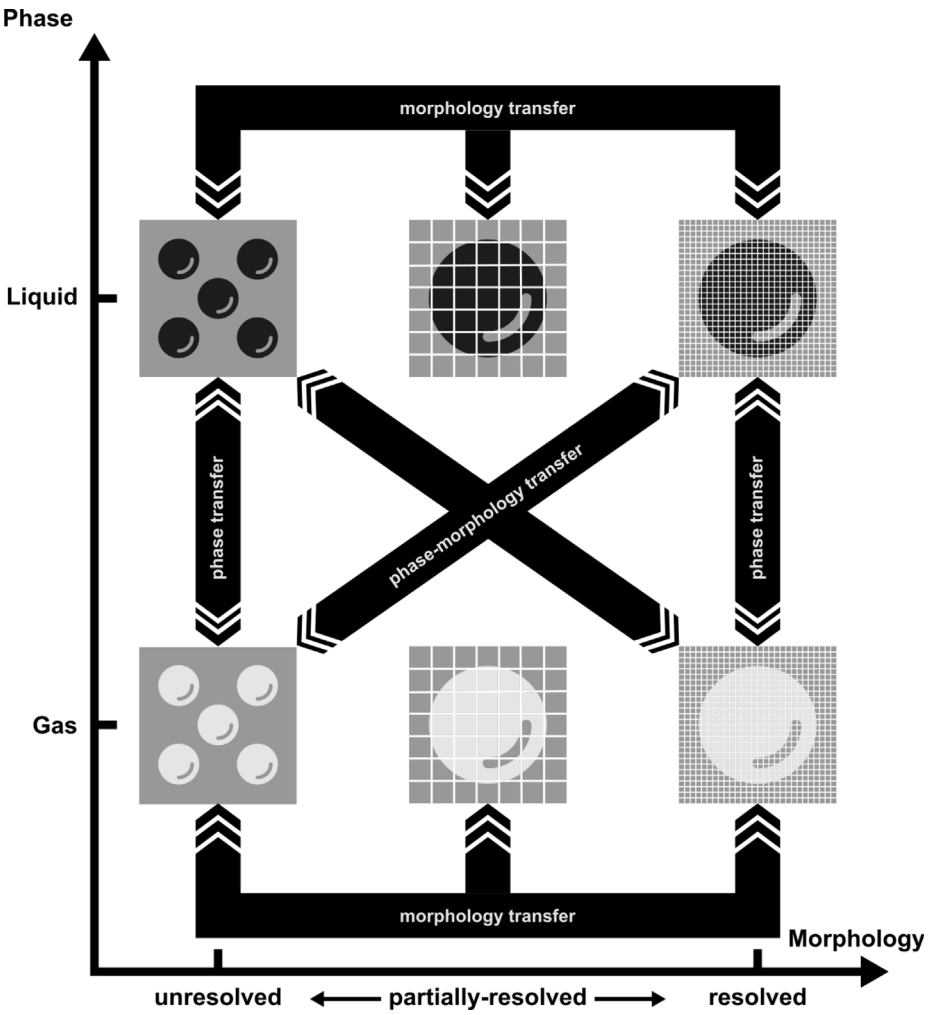

Fig. 5. Sketch of possible transfer between physical phases and morphologies in a morphology-adaptive Eulerian method. The term 'transfer' includes mass, momentum and energy transfer.

as the fluid is composed of several numerical phases k, we define a phase indicator function for any realization γ, as

$$X_k(\mathbf{x},t,\gamma) = \begin{cases} 1 & \text{if } k \text{ is present at point } \mathbf{x} \text{ at time } t \text{ in realization } \gamma, \\ 0 & \text{otherwise.} \end{cases} \tag{2}$$

The ensemble average of the phase indicator function provides the expected value of the ratio between the volume of numerical phase k and the total volume, in the limit that the volume approaches zero. Or in other words, the probability of finding phase k at point $\mathbf{x}$ and time t. This quantity is well-known and typically named phase fraction, volume fraction, or void fraction.

$$\alpha_k = \langle X_k \rangle \tag{3}$$

The phase-average is defined as

$$\tilde{f}_k = \frac{\langle f_k \rangle}{\alpha_k} \tag{4}$$

and the mass-weighted (Favre) average as

$$\overline{f}_k = \frac{\langle \rho_k f_k \rangle}{\langle \rho_k \rangle} = \frac{\langle \rho_k f_k \rangle}{\alpha_k \tilde{\rho}_k}. \tag{5}$$

In case the observable f is not defined specifically for a phase k, the value for f_k is obtained by taking the value of f only into account in case the phase k is locally present, i.e., the phase-specific value of the observable is obtained from $f_k = X_k f$. With this relation, Eqs. (4) and (5) are valid regardless of the chosen averaging procedure denoted by $\langle . \rangle$. The phase-averaged mass conservation equation then reads as

$$\frac{\partial \alpha_k \tilde{\rho}_k}{\partial t} + \nabla \cdot (\alpha_k \tilde{\rho}_k \overline{\mathbf{v}}_k) = \Gamma_k \tag{6}$$

where $\tilde{\rho}_k$ is the phase-weighted density, and $\overline{\mathbf{v}}_k$ the mass-weighted velocity. The right-hand side of Eq. (6) represents the linearized interfacial mass generation source Γ_k [15]

$$\Gamma_k = \sum_{l=1}^{n} \left(\dot{m}_{lk} - \dot{m}_{kl} \right), \tag{7}$$

where $\dot{m}_{lk}$ and $\dot{m}_{kl}$ represent the mass transfer from the lth phase to kth phase and vice versa, and n represents the total number of numerical phases. It is also defined that $\dot{m}_{kk} = 0$. Eq. (7) implies, that the mass exchange terms sum-up to zero ($\sum_{k=1}^{n} \Gamma_k = 0$).

The phase-averaged momentum conservation equations can be derived in the same manner

$$\frac{\partial \alpha_k \tilde{\rho}_k \overline{\mathbf{v}}_k}{\partial t} + \nabla \cdot (\alpha_k \tilde{\rho}_k \overline{\mathbf{v}}_k \overline{\mathbf{v}}_k) = -\alpha_k \nabla \tilde{p}_k + \nabla \cdot \left(\langle \boldsymbol{\tau}_k \rangle + \langle \boldsymbol{\tau}_k^{\mathrm{Re}} \rangle \right) + \alpha_k \tilde{\rho}_k \mathbf{g} + \mathbf{M}_k + \Omega_k \tag{8}$$

where $\mathbf{g}$ is the gravitational vector, $\mathbf{M}_k$ represents the interfacial momentum exchange terms, e.g., lift, virtual mass, drag, and contains information that is lost due to averaging [10]. The stresses include the phase pressure p_k, the viscous stresses τ_k and the (turbulent) Reynolds-stress $\langle \boldsymbol{\tau}_k^{\mathrm{Re}} \rangle$. The last term in the right hand side defines the linearized

interfacial momentum source due to mass transfer, Ω_k [15]

$$\Omega_k = \sum_{l=1}^{n} \left(\dot{m}_{lk} \mathbf{v}_l - \dot{m}_{kl} \mathbf{v}_k \right). \tag{9}$$

The momentum sources induced by mass transfer, Ω_k, and the interfacial momentum terms, $\mathbf{M}_k$, balance across all existing phases ($\sum_{k=1}^{n} \Omega_k = 0$ and $\sum_{k=1}^{n} \mathbf{M}_k = 0$). In a stagnant flow, the individual phase pressures $\tilde{p}_k$ match such that $\tilde{p}_k = \tilde{p}$. It is common practice to assume that this equality of the phase pressures is still valid in dynamic scenarios, and required for solving Eqs. (6) and (8) (shared pressure assumption). As an alternative individual phase pressures can be taken into account, e.g., by adding derivations from the average pressure $\tilde{p}_k - \tilde{p}$ to Eq. (8). Note that the energy equation is not discussed here, as our present focus is on isothermal fluids and their hydrodynamics.

As already mentioned in the introduction, within industrial applications unresolved and resolved morphologies are allowed to occur simultaneously. In the following we will demonstrate that under special circumstances, Eqs. (6) and (8) reduce to the well known homogeneous or Volume-of-Fluid model. Hence, it is possible to treat resolved morphology in a Volume-of-Fluid sense with the same set of equations originally derived for unresolved morphologies, which opens up the possibility to develop morphology-adaptive Eulerian methods. First, we sum up the phase-averaged mass conservation equations for all phases k (Eq. (6)). This yields the conservation equation for the total mass, the so-called mixture mass conservation

$$\frac{\partial \rho_\mathrm{m}}{\partial t} + \nabla \cdot (\rho_\mathrm{m} \overline{\mathbf{v}}_\mathrm{m}) = 0. \tag{10}$$

The right-hand side of Eq. (6) sums up to zero for all phases. The mixture quantities with subscript m are defined as

$$\rho_\mathrm{m} = \sum_{k=1}^{n} \alpha_k \tilde{\rho}_k \qquad \text{and} \tag{11}$$

$$\mathbf{v}_\mathrm{m} = \frac{1}{\rho_\mathrm{m}} \sum_{k=1}^{n} \alpha_k \tilde{\rho}_k \overline{\mathbf{v}}_k. \tag{12}$$

The same is possible for the phase-averaged momentum equations (Eq. (8))

$$\frac{\partial \rho_\mathrm{m} \overline{\mathbf{v}}_\mathrm{m}}{\partial t} + \nabla \cdot (\rho_\mathrm{m} \overline{\mathbf{v}}_\mathrm{m} \overline{\mathbf{v}}_\mathrm{m} + \mathbf{J}) = -\nabla p_\mathrm{m} + \nabla \cdot \left(\langle \tau_\mathrm{m} \rangle + \langle \boldsymbol{\tau}_\mathrm{m}^\mathrm{Re} \rangle \right) + \rho_\mathrm{m} \mathbf{g}, \tag{13}$$

where $\mathbf{J}$ is the so called drift flux tensor (slip tensor):

$$\mathbf{J} = \sum_{k=1}^{n} \alpha_k \tilde{\rho}_k \left(\overline{\mathbf{v}}_k - \overline{\mathbf{v}}_\mathrm{m} \right) \left(\overline{\mathbf{v}}_k - \overline{\mathbf{v}}_\mathrm{m} \right) \tag{14}$$

Note that surface tension is neglected here for simplicity, but can be added at any time using the approach of Brackbill et al. [16]. The mixture equations for the homogeneous model (or Volume-of-Fluid) can be obtained by setting $\mathbf{J} = 0$, which implies equal velocities for all phases k. This reveals the central role of slip between a pair of phases: allowing for a relative velocity means to move away from the Volume-of-Fluid-like representation of the interface.

As a hypothesis for the development of morphology-adaptive Eulerian methods we assume that it is possible to obtain one realization γ for an interface between a given pair of continuous phases from the phase-averaged equations (Eqs. (6) and (8)), if

- an interfacial closure model $\mathbf{M}_k$ exists, that ensures $\mathbf{v}_k = \mathbf{v}_l$ (no slip) for two phases sharing the interface, and
- it is possible to recreate an interface by introducing information that has been removed by averaging before, e.g., shape and location of the interface.

Such a realization of an interface can be interpreted as a switching process from a stochastic to a deterministic representation.

This also defines the so-called edge cases for the morphology-adaptive Eulerian methods, which are the homogeneous (Volume-of-Fluid) model for high mesh resolutions (right side of Fig. 4) and the Euler-Euler model for low mesh resolutions with appropriate closure models (left side of Fig. 4). Hence, the phase-averaged conservation equations form a useful basis for a morphology-adaptive method, which can be considered as an extension of the Euler-Euler model. Because it is possible to change from a stochastic (averaged) representation to a deterministic (resolved) representation, engineers can investigate multiphase flows with more details, hopefully helping them to optimize applications further. However, the simulation will contain only one specific realization of the interfaces out of an infinitely large ensemble.

2.3. Turbulence modeling

In the following we will briefly visit the complex topic of modeling strategies for turbulence in multiphase flows, and some of the specific issues that are encountered when modeling it in morphology-adaptive Eulerian methods. The difficulty arises from the fact that turbulent scales and interfacial scales are often not in the same range, even though they heavily interact with each other, e.g., turbulent eddies near an interface influence the heat transfer and in turn condensation and evaporation processes. As a morphology-adaptive Eulerian method is developed mainly for engineering scale simulations, (fully) resolving turbulent scales is neither intended nor feasible. More within reach, at least for some applications, is the partial resolution of the turbulent scales, like in large-eddy simulations. There the flow fields are filtered, and thus modeling is required only for the unresolved (subgrid) turbulent scales. Attempts in this direction have been made by e.g., [17–20]. At the moment, the most often used approach has been the full modeling of the turbulent scales, e.g., by a Reynolds-Averaged Navier–Stokes (RANS) two-equation approach, a zero-equation model, or Reynolds stress modeling. Well-known for the Euler-Euler model is the influence of an unresolved morphology on the turbulence of a resolved morphology of another physical phase, i.e., the so-called induced turbulence by bubbles, droplets or particles [21]. The same holds for the influence of a resolved morphology on the turbulence of a unresolved morphology of another physical phase, i.e., turbulent dispersion, aggregation, coalescence, breakup, and entrainment.

Morphology-adaptive Eulerian methods add the complexity of having to model the turbulent interactions between two resolved morphologies, which is the subject of investigation in particular for nuclear safety applications, e.g., accident scenarios where stratified flows are present, such as the aforementioned pressurized thermal shock (Fig. 2). The problem arises when the interface can be reasonably well resolved, but the grid is still much too coarse for fully resolving the turbulent eddies near the interface. RANS models tend to over-predict the turbulent production near interfaces, due to typically high velocity gradients there. This is known already from near-wall turbulence modeling, and, hence, several researchers introduce a damping source term in the turbulence equations with a near-wall analogy in mind [22–29]. However, recent work for modeling turbulent multiphase flows with the homogeneous model and mixture turbulence (i.e., not per phase turbulence) shows that a reasonable prediction can be achieved without such a wall-like damping term near the interface, if the turbulence model is formulated ‘correctly’, i.e., with a density formulation [30–33]. So far those modeling strategies have not yet been applied to morphology-adaptive Eulerian methods. However, the usage of state-of-the-art RANS models for morphology-adaptive Eulerian methods is relatively straightforward: For an unresolved morphology additional source terms for induced turbulence are required, e.g., [21], and for a resolved morphology a turbulence damping model near the interface should be employed, e.g., [22,26]. The remaining challenge is to identify the interface in blended methods to apply the damping term correctly. For separated methods the interface is usually well-defined due to the distinction in different numerical phases.

An additional challenge for morphology-adaptive Eulerian methods is treating waves. Waves of various heights can emerge from flow instabilities at the interface if the velocity difference is large enough.

The modeling of waves becomes more difficult because they have to be distinguished into unresolved and resolved waves, which can also influence each other. Pedroso et al. [34] have used the MultiMorph model (see Section 3.4 for details) as a basis and developed the so-called Modified Mixture Model. Their approach shows robustness across mesh refinements and effectively captures the wave dynamics and other key wave characteristics. Höhne and Hänsch [35] proposed another source term for the turbulence equations to take into account the effect of small waves, which counter-acts the wall-like turbulence damping. It remains subject to future investigations if such a modeling strategy is promising.

The discussion above reveals that the topic of turbulence in multiphase flows is tremendously more complex than for single phase flows, as a result of the presence of a phase interface. It will be an endeavor to include all physically relevant turbulence effects into morphology-adaptive Eulerian methods. Hence, it shows the importance of laying out the fundamentals for modeling hydrodynamics and the interaction between the morphologies as we attempt in this publication, to achieve some common agreement and steer future developments.

2.4. Performance and accuracy

The basic idea of morphology-adaptive Eulerian methods is to address the limitations that arise when multiphase flows exhibit different morphologies or flow regimes, such as dispersed and segregated structures, spanning a large range of scales or featuring morphologies that are not known a priori. These methods are primarily designed for engineering applications, where robustness and flexibility play an important role. It is important to emphasize that morphology-adaptive Eulerian methods do not inherently improve the accuracy of the simulation results in the limits of unresolved and resolved morphologies. For unresolved morphologies, the achievable accuracy is still governed by the selected closure models, in the same manner as for the conventional Euler-Euler model [10]. Likewise, for resolved morphologies, the accuracy is comparable to that of Volume-of-Fluid methods. The same limitation applies to physical sub-models, such as bubble breakup and coalescence. Hence, morphology-adaptive Eulerian methods do not overcome any known deficiencies of either classical Euler–Euler or Volume-of-Fluid methods in this context. The main advantage in terms of accuracy is the ability to use the optimal modeling strategy for resolved and unresolved morphologies and to change between them dynamically during the simulation. This extends the range of applicability of multiphase flow simulations and yields new possibilities for modeling them. However, it should be noted that for partially-resolved morphologies information on the interface will get lost in case the structure disintegrates, and information has to be restored in case of coalescence or growth. A typical design criterion is a fast and robust transition algorithm, which tries to preserve a minimum number of quantities, e.g., the bubble rise velocity [36] or tries to avoid nonphysical peaks in the void fraction [37]. Morphology-adaptive Eulerian methods are not developed to overcome model limitations — they should manage them.

From a performance perspective, morphology-adaptive Eulerian methods are based on the Euler-Euler model and require at least one numerical phase per physical phase. This requirement introduces an increased numerical overhead, which generally makes these methods slower than Volume-of-Fluid approaches at a given computational mesh. A blended method may, depending on the specific implementation, achieve computational performance comparable to regular Euler-Euler model, as no additional numerical phases are introduced in this case. The separated methods, however, may again be slower than blended methods due to the presence of additional numerical phases associated with the explicit representation of different morphologies. A first glimpse into the performance characteristics and comparative computational cost of morphology-adaptive Eulerian methods can be found in [38]. Further computational overhead may arise from closure models applied at resolved interfaces, which can lead to stiff systems of partial-differential equations, as discussed by Meller et al. [39]. Additional costs may also originate from the interface detection techniques required for blended methods. Overall, a clear performance trade-off exists: a computational penalty must be paid as the price for the enhanced flexibility provided by morphology-adaptive Eulerian methods.

3. Available implementations

After the terminology and basic equations have been introduced in Section 2, this section presents different implementations which were developed by organizations associated with the Dresden6 group. This includes open-source as well as commercial software packages. An overview about the licenses, the developing organizations and the availability is given in Table 1. In the following each implementation is briefly introduced and literature references are given for further details.

3.1. Generalized multifluid modeling approach

The Generalized Multifluid Modeling Approach (GEMMA) extends the solver for the Euler-Euler model in the software released by the OpenFOAM Foundation (named *multiphaseEuler*). It implements a methodology to detect resolved morphologies, and models continuous intermittent phase structures and segregated flows [40,41]. GEMMA is a blended method and solves a single set of conservation equations, for all morphologies of each physical phase. The resolved morphologies are marked by a scalar field, which is equal to 1 in cells occupied by a large interface, and 0 in regions with unresolved morphology or inside phase regions that are already continuous. The marker is calculated by an estimation of the length scale of the resolved morphology and the resolution of the interface curvature allowed by the computational grid, quantified by an interface resolution quality parameter. Furthermore, the marker takes into account the characteristic size of the unresolved morphology, identified from the Sauter-mean diameter, or the local volume fraction gradient. If the criteria for a resolved morphology are met, a dedicated formulation for those morphologies is activated. This includes a numerical compression flux, normal to the interface and proportional to the relative velocity between the phases, to keep the interface sharp [42]. A blending methodology between resolved and unresolved morphologies ensures that proper closures are applied. The blending is achieved by superimposing the marker scalar field to the native blending functions available in the software released by OpenFOAM Foundation. GEMMA can be coupled with the class-based population balance model, available RANS turbulence models, with bubble induced turbulence and the wall-like turbulence damping approach mentioned before. The model has been validated against several different test case in [40] and already employed to predict stratified flows [41], cross-flow in a steam generator tube bundle [43], multiphase flows with heat transfer and phase change [44] and flow regime development and transition in a horizontal pipe [45].

3.2. Generalized two-phase flow concept

The Generalized Two-phase Flow Concept (GENTOP) was first introduced by Hänsch et al. [46,47]. The concept is applied as a three-field method solving a set of conservation equations for an unresolved and a partially-resolved dispersed phase (either gas or liquid), and a resolved continuous phase (either liquid or gas respectively). The class-based population balance model is extended by a partially-resolved dispersed phase, which by definition exceeds a certain bubble or droplet diameter-to-grid size-ratio and for which a blending of closure models according to the detected dispersed phase morphology is applied. Hence, GENTOP can be considered a combination of a blended method and a separated method. The original model was implemented in Ansys

Table 1
Overview of available implementation of morphology-adaptive Eulerian methods in Dresden6 group.

Method	Organization(s)	License	Requirement(s)	Availability
Generalized Multifluid Modeling Approach (GEMMA)	University of Sheffield	GPL-3.0-or-later	OpenFOAM Foundation Software 9 and additional code	Upon request
Generalized Two-phase Flow Concept (GENTOP)	Helmholtz-Zentrum Dresden-Rossendorf e.V. and Ansys Germany GmbH	Proprietary	Ansys Fluent 23R2, Ansys CFX 13	https://www.ansys.com
Hybrid Dispersed and Four Field Large Interface Solver (HD-LIS/FF-LIS)	NRG PALLAS	GPL-3.0-or-later	OpenFOAM Foundation Software 9 and additional code	https://github.com/edofrederix/fourFieldLIS
Morphology-adaptive Multifield Euler-Euler Model (MultiMorph)	Helmholtz-Zentrum Dresden-Rossendorf e.V.	GPL-3.0-or-later	OpenFOAM Foundation software development line and Multiphase Code Repository by HZDR	https://doi.org/10.14278/rodare.767
Algebraic Interfacial Area Density Model (AIAD)	Helmholtz-Zentrum Dresden-Rossendorf e.V. and Ansys Germany GmbH	Proprietary	Ansys Fluent 23R2, Ansys CFX 11	https://www.ansys.com
Large-Scale Interface Model (LSI)	Siemens Industry Software	Proprietary	Simcenter STAR-CCM+	https://www.siemens.com

CFX 13 via user-defined functions, but is now part of the official Ansys Fluent since version 23R2. In this version, the GENTOP model does not impose any restrictions on the state of the dispersed or continuous phases: it can also handle droplets in continuous gas and capture the inception of continuous liquid phase (the so-called GENTOP phase).

Resolved interfaces are detected via a critical volume fraction gradient of the partially-resolved dispersed phase based on the grid resolution. The morphology of the partially-resolved phase is further defined via volume fraction limits, which, when exceeded, activate two transfer mechanisms that transfer the dispersed phase from unresolved to resolved morphology: an additional interfacial "clustering" force opposing the continuous phase volume fraction gradient that aggregates all dispersed phase volume fraction when a certain volume fraction limit is reached, and a "complete coalescence" transferring all remaining unresolved dispersed phase fractions to the resolved phase. Introducing these transfer mechanism the GENTOP model does not only allow the simulation of mixed flow regimes, but also the transition from one morphology to another.

The mass transfer between unresolved and resolved morphologies, including the appearance and disappearance of a particular phase, was demonstrated for an impinging jet, a bubble column and a dam break case [46,47]. Later the model was applied to high-void fraction regimes (churn-turbulent and slug flow) in a vertical pipe [48] and supplemented with a suitable surface tension model [49]. More recently, flow regime transitions were simulated in heated pipes [50] and a new wall boiling model was coupled by Setoodeh et al. [51].

3.3. Hybrid dispersed and four field large interface solver

The Hybrid Dispersed Large Interface Solver (HD-LIS) presented by Mathur et al. [52] is a blended method based on the Euler-Euler model in the software released by the OpenFOAM Foundation (named *multiphaseEuler*). In HD-LIS, each physical phase is represented by a single volume fraction field (i.e., a numerical phase). A flow regime map, constituted by hyperbolic tangents, is used to determine the local morphology based on the volume fraction field. Depending on the identified morphology, appropriate interfacial closure models are applied, and blending functions are used to ensure smooth transitions between the different morphologies. Additionally, a numerical compression flux is added in the regions where a resolved morphology is identified, to counteract the numerical smearing of large interfaces [42]. For turbulence modeling near large interfaces, HD-LIS adopts the turbulence damping approach of Frederix et al. [26], which was introduced above, in Section 2.3.

The Four Field Large Interface Solver (FF-LIS) was introduced by Frederix et al. [53] as an extension of the HD-LIS model and features a separated method. In FF-LIS, two physical phases are represented by four numerical phases, introducing a formal separation between resolved and unresolved morphology of each phase. Because of this, each pair of numerical phases can adopt different closures, removing the need for blending functions. Instead, the key to the FF-LIS becomes the appropriate and accurate modeling of phase and morphology transfer terms for mass, momentum and energy. In [53], a morphology transfer model is introduced for FF-LIS, which accounts for mass transfer from the resolved morphology to the unresolved one due to break-up of interfacial structures, as well as from the unresolved morphology to the resolved one due to coalescence of unresolved interfacial structures among themselves, or due to absorption of unresolved interfacial structures into a resolved interface.

Both HD-LIS and FF-LIS rely on the LogMoM model for the description of the particle population, in either physical phase [54,55]. The LogMoM model assumes a log-normal size distribution and handles unresolved morphology break-up and coalescence in a generic way, handling any given break-up or coalescence kernel.

3.4. Morphology-adaptive multifield Euler-Euler model

The Morphology-adaptive Multifield Euler-Euler Model (MultiMorph) belongs to the separated methods, i.e. each morphology is represented by a dedicated numerical phase (no blending between morphologies, Schlegel et al. [56]). The interfacial closure models are selected according to the local morphology. For unresolved morphologies the baseline strategy by HZDR is applied [57]. For a resolved morphology, $\mathbf{J} = 0$ is achieved by a tight coupling according to Štrubelj and Tiselj [58]. The partially-resolved morphologies are treated by an adaptive coupling, based on an under-resolution indicator allowing $|\mathbf{J}| \geq 0$ [36]. The coupling adapts to the local mesh resolution, e.g., if the local mesh resolution is sufficiently high, unresolved morphologies are subject to a coarsening treatment to avoid non-physical results [37], before they are turned into a resolved morphology with a morphology transfer [59]. On the other hand, if the mesh resolution is too low, resolved morphologies are transferred into unresolved morphology [60]. Note that the resolution requirements for the morphologies are significantly relaxed because of the adaptive coupling mentioned above. Those resolution-adaptive transfer formulations are independent from the time step size. The whole framework is designed to allow precise control of the coupling and the transfers between the physical and numerical phases. The disadvantage is that those transfers have to be organized carefully to ensure that all degrees of freedom are determined and to keep the framework stable. The MultiMorph method is available open-source as additional source code for the OpenFOAM Foundation software [61]. It has been applied for several test scenarios, e.g., a rising bubble in stagnant liquid [20,39], or stratified-flows [28,36]. It also shows promising results for complex applications like a gas–liquid separators [62,63], droplet entrainment in annular flows [64], column trays of a distillation column [65], or air-lubrication in naval vessels [66].

3.5. Algebraic interfacial area density model

The Algebraic Area Density Model (AIAD) deploys blending functions dependent on phase volume fractions as well as volume fraction gradients for morphology detection, and, hence, belongs to the blended methods. The model does distinguish between three different morphologies: droplets, bubbles and a free surface. Different closure laws for interfacial area and drag can be applied to each morphology weighted by blending functions

The AIAD model is equipped with an interfacial surface drag law which considers the free surface as free shear layer and hence relies on the interfacial viscous shear stress tensor and volume fraction gradients. The AIAD model was proposed by Egorov [22] to enhance the predictive capabilities of Eulerian multiphase models when dealing with intermittent flow regimes with multiple morphologies. Since then, it has been successfully deployed in wide range of applications such as in the simulation of counter current two-phase flow in the hot leg of a pressurized water reactor by Höhne and Mehlhoop [23]. The model has been compared intensively to experimental data of the WENKA and HAWAC test facilities [23,67] respectively.

The model has evolved since its first development as many improvements have been made to it, particularly in the areas of phase transition, free surface drag function and turbulence damping at the gas–liquid interface. The AIAD model as implemented in Ansys Fluent does feature two additional ingredients on top of its core regime blending capability. The first ingredient accounts for sub-grid wave turbulence generation due to the impact of tiny unresolved interfacial waves on the liquid phase's turbulent kinetic energy. The second ingredient is related to entrainment and absorption of secondary droplets. These droplets are first generated due to the destabilization of the interface by turbulence. Entrained droplets can deposit back on the liquid interface and merge with the continuous liquid phase. A population balance model can also be used in conjunction with AIAD to monitor the size distribution of droplets suspended in the continuous gas flow. A detailed description of the entrainment model can be found in the work of Höhne and Hänsch [35]. At last, the AIAD model implementation in Ansys Fluent relies on the Multi-Fluid VOF technology and deploys the flow regime aware volume fraction interpolation algorithm to sharpen the interface wherever it is necessary.

3.6. Large-scale interface model

The Large-Scale Interface Model (LSI) was developed by Gada and Eliasm [68] and Gada et al. [25] with the objective of extending Siemens STAR-CCM+ towards a morphology-adaptive Eulerian method capable of simulating applications with coexisting flow regimes. The LSI model generally relies upon a criterion based on local phase distribution to demarcate flow into three distinct regimes – two dispersed and one interfacial – and, hence, is a blended method. Appropriate closures for exchange terms appearing in transport equations of the conserved variables are specified for each regime, and a weighted sum of individual closures determines the final exchange term.

Since its introduction, the model has seen numerous advancements. Gada et al. [69] extended the LSI model by introducing a procedure to dynamically detect large-scale interfaces within the domain based on the work of Coste [70]. The procedure is capable of being used for problems involving multiple physical phases, identifies a single cell-thick interface and pre-specified thick layers of cells on either side of the interface. The capability to detect free surfaces enabled the development of the Adaptive Interface Sharpening (ADIS) scheme [29]. The ADIS scheme was developed to adaptively use an interface sharpening scheme of choice near the free surface for the transport of volume fraction and a TVD scheme of choice away from the interface. Tandon et al. [29] demonstrated that the scheme is more accurate for applications with coexisting flow regimes, as it can maintain the sharpness of the large-scale interface over a period without causing any artificial sharpening within the dispersed regime.

The interface detection procedure was extended by Gada and Tandon [71] to provide the distance of cells from the detected interface using the interface reconstruction procedure of Rider and Kothe [72]. This extension allowed the LSI model to use wall-function-based turbulence damping for free surfaces, as it is known to be mesh-independent. For this purpose, a stencil based on the work of Coste and Laviéville [73] was used for each interface cell. The stencil consists of an interface cell and a cell on either side of the interface with a knowledge of the phase occupying those cells. No special treatment is done for the interface cell, while wall-function-type damping is applied in the cells on either side of the interface. It has been shown that such a treatment requires no special tuning for different meshes or problems. Gada and Tandon [74] coupled the LSI model with the moments-based population balance model implemented in Siemens STAR-CCM+ [75], wherein they developed a methodology based on the work of Brocchini and Peregrine [76] to identify cells where the conditions lead to the rupture of the free surface. The methodology uses the work of Yu et al. [77] to determine the size of dispersed particles detaching from the interface post its rupture.

4. Tests for method homogenization

To start a homogenization process is important for the broad application of morphology-adaptive Eulerian methods in industrial design and licensing processes. The idea of the following chapter is to lay down the fundamentals for such a homogenization process by defining a set of separated effect and integral tests. The presented collection is based on the test cases already simulated by the members of the Dresden6 initiative and accompanied with literature cases. The collection will be extended in the future towards a homogenization database to proof the capabilities of morphology-adaptive Eulerian methods and to serve as a benchmark for cross-comparison. It should be noted that not all presented test cases have been simulated by all simulation frameworks presented in Section 3 yet.

4.1. Separated effect tests

Separated effect tests should be focused on one or only a few representative phenomena, which can be distinguished from each other in the simulation results. An important feature of such tests is robustness, which means that complex interactions between different phenomena should be avoided, and the tests should have well-defined initial conditions and boundary conditions, and ideally many measured flow parameters or an analytical solution as a reference. Their aim is to provide sufficient data for testing if the developed models, e.g., closure laws, transfer models, or turbulence models accurately represent the expectations and the reality faithfully.

A well-known flow example, which serves as a separated effect test, are stratified channel flows. The geometry is typically a horizontal channel with a rectangular or circular cross-section. At least two fluids, separated by gravity due to different densities, are streaming in either co-currently (same flow direction), or counter-currently (opposite flow direction). Three different flow regimes can appear, which are smooth interface, wavy interface and slug formation. Stratified channel flows allow to investigate the behavior of the resolved morphology and the partially-resolved morphology, including the respective drag modeling. Very important effects are the turbulence near interfaces and the onset and the development of waves. For a laminar stratified two-phase shear flow an analytical solution has been presented by Marschall [78] and the simulation results of Mathur et al. [52] show a good agreement. One of the most used experimental data for smooth and wavy surfaces in stratified channel flows has been presented by Fabre et al. [79]. Quantitative experimental data is available, however, the most important data close to the free surface is missing. Coste et al.

[80], Coste [70], Coste and Laviéville [73], Mathur et al. [52], Colombo et al. [41,81], Meller et al. [36] and Höhne and Mehlhoop [23] have simulated this channel flow successfully.

The best experimental stratified channel flow data currently available stems from the WENKA (Water Entrainment Channel Karlsruhe) experiments of Stäbler [82]. Mainly counter-current flows have been investigated with smooth and wavy surfaces. The available data includes velocity profiles for several cross-sections, turbulence data in the interface region and the pressure drop. Tekavčič et al. [28], Schlegel et al. [56] and Yan et al. [83] have simulated the WENKA test facility for the operating points of smooth interfaces and obtained reasonable results.

Wavy flows in a channel represent an important separated effect test and should be used to study the fundamental mechanisms on wave formation and growing in morphology-adaptive Eulerian methods. Fleau [18] and Štrubelj and Tiselj [84] have simulated an old experiment by Thorpe [85], who investigated the formation of basic Kelvin–Helmholtz instabilities in stratified shear flow. Höhne and Mehlhoop [23] simulated co-current wavy cases in Horizontal Air/Water Channel (HAWAC, Vallée et al. [86]) and Fabre et al. [79] using the AIAD model (Section 3.5). Coste et al. [80] used the large interface model in Neptune_CFD to simulate co-current wavy cases from air–water experiments of Fabre et al. [79] and steam-water experiments of Lim et al. [87].

For the slug flow regime in horizontal channels not many CFD-grade experiments are available, e.g., some data is available from the HAWAC experiment by Vallée et al. [86]. Recently, Friedemann et al. [88] have presented another experiment, which has been simulated by Colombo et al. [41]. However, as only the mixture velocity is available, the comparison between simulation and experiment is difficult.

The well-suited separated effect test for multiphase flows in general is the **single bubble**. Single bubbles are studied extensively in numerical simulations [89–93], and define an edge-case for morphology-adaptive Eulerian methods. Their main task is to confirm that resolved morphologies can be predicted well on a sufficiently fine grid, including surface tension and interface sharpening (Fig. 6(a)). For almost every simulation framework presented in Section 3, simulation results for a single bubble in stagnant liquid are available [18,39,39,40,52,53,56]. Beyond that they can be used to analyze several mesh-related effects, like the prediction of partially-resolved morphologies on medium sized meshes, or the transfer from resolved to unresolved morphology and back depending in local mesh size (see Fig. 6(b)). For instance Meller et al. [36] developed a resolution-adaptive drag model on coarsely resolved interfaces, and further extended their morphology-adaptive Eulerian method with a transition between deterministic and stochastic representation, by simulating the rise of a single bubble through regions of different mesh resolution. It is also possible to combine a single bubble with dispersed bubbles and let them rise together [39,94].

A **Taylor bubble** rises in a vertical pipe, which yields several interesting effects, like a thin-film flow between the large Taylor bubble and the wall, breakup of the Taylor bubble in the wake, entrainment of small bubbles and other turbulent wake effects (see Fig. 6(c)). Recently new high-resolution experimental data has been published by Mikuž et al. [95,96], Kren et al. [97], Tiselj et al. [98], and Kren et al. [99]. They investigate the dynamics of a Taylor bubble in a vertical counter-current flow, which allows to keep the bubble stagnant in the observation window. An interface recognition algorithm is used to determine the bubble interface from 2D shadowgraphy measurements. The experimental data includes bubble shape, bubble position, film thickness and interface disturbance waves (z-axial velocity, frequency-power spectra). The experiment has been simulated already by Frederix et al. [100] and Kren et al. [101] using DNS and LES respectively. The Taylor bubble case is very suitable for numerical simulation because the bubble can be made stagnant in counter-current flow (as was experimentally done), or can be simulated in a moving reference frame attached to the bubble. At the same time, by controlling the relevant non-dimensional numbers, the complexity of the problem in terms of bubble break-up, coalescence, film thickness, wake turbulence and turbulence at the interface can be easily adjusted.

4.2. Integral tests

Integral tests increase the complexity by combining more than a few phenomena together. The intent is to verify that all mechanisms work well together and that all important phenomena are modeled by the developed morphology-adaptive methods. They are a prerequisite for reproducible modeling of complex industrial applications.

An interesting example is the **bubble column**, which is typically simulated with an Euler-Euler model and a degassing boundary condition at the top [38]. Direct numerical simulations are very challenging and only a few are available, e.g., [102]. Within those simulations the focus is mainly on developing interfacial closures for e.g., drag, virtual mass and lift. However, they can be extended as an integral test for morphology-adaptive Eulerian methods by including the free surface or by refining the mesh to resolve the bubbles. Depending on the operating conditions, several phenomena can be investigated together, e.g. waves at the free surface, bubble bursting at the free surface, and bubble coalescence. It is also possible to use artificially increased coalescence to create large gas bubbles that can be treated as resolved morphology. This has already been done successfully by Hänsch et al. [46] and Frederix et al. [53].

Frequently studied, and well qualified for an integral test, are **plunging jets**. In these tests, a liquid jet hits a basin of liquid and a bubble plume is formed due to entrainment of gas from above the surface. The free surface typically forms waves, and both bubbles and droplets can be generated. Hence, multiple morphologies interact with each other and require robust and reliable transfers. Inside the bubble plume breakup and coalescence will take place, increasing the challenge for the morphology-adaptive Eulerian methods. Several experiments are available [103–106], including measurements with ultra-fast X-ray tomography, which allows to determine the bubble size distribution [107]. Simulations have been performed by several authors, e.g., [40,46,52,53,70,73,80,108,109].

When experiments cover both dispersed and segregated regimes and their co-existence, **channel flows** can serve as integral tests as well. For example in the METERO experiment by Bottin et al. [110] a bubbly flow is used instead of a stratified one, and the transition to the plug, slug and stratified regimes is studied. This creates several complex interactions between the morphologies and conditions that are challenging for morphology-adaptive Eulerian methods, which need to handle the transition from unresolved to resolved morphology and their co-existence. Flow regime transition, e.g., from smooth to wavy or from bubbly to slug flow greatly increase the complexity and can require the coupling to a population balance model. Simulation results with morphology-adaptive Eulerian methods are available by Mathur et al. [52], Frederix et al. [53], Colombo et al. [81] and Colombo and Fairweather [45]. Introducing an orifice into the horizontal channel yields new phenomena like droplet generation and deposition behind the obstacle. Experimental data is available for horizontal channel flows with an obstacle by Weise et al. [111] and Porombka et al. [112]. Going away from flat horizontal channels towards L-shaped channels, allows to look into waves, droplet generation and entrainment. Experimental data is available from the WENKA test facility [113] and has been simulated already by Höhne and Gabriel [114]. Finally, the channel can be turned into a vertical channel, which allows to study regime transitions from bubbly to churn-turbulent and slug flow as well and changes the influence of the gravity on the phase distribution. Experimental data is available from the Transient Two Phase Flow Test Facility (TOPFLOW) together with a systematic analysis by Lucas et al. [115]. Those cases have been simulated by Montoya et al. [48,49] with the GENTOP model (Section 3.2).

Černe et al. [116] proposed another interesting test case for analyzing morphology-adaptive Eulerian methods with respect to transfer modeling, and this is the so-called Rayleigh–Taylor Instability. The case setup is described in detail by Canot and Vincent [117]. Štrubelj [118] proposed this as a two-dimensional benchmark, and it has been simulated by Štrubelj and Tiselj [58,84], Rezende et al. [119] and Fleau [18]. However, there is no experimental data available.

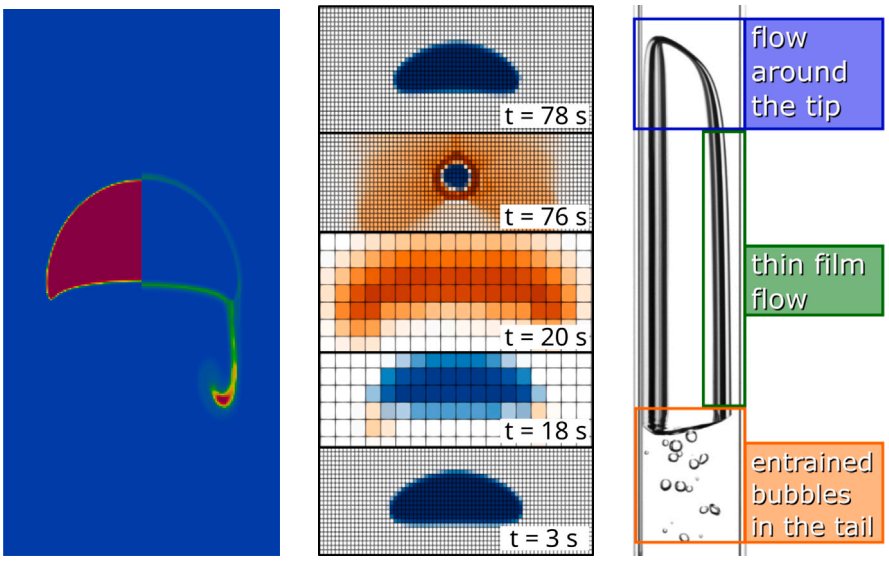

(a) Single rising bubble. (b) Transition of a single rising bubble. (c) Taylor bubble.

Fig. 6. (a) Simulation results from morphology-adaptive Eulerian methods for the second case of Hysing et al. [89] on a sufficiently fine grid with the left half showing the resolved morphology and the right half showing the unresolved morphology showing a small amount of break-up. (b) Snapshots of the transition of a single bubble from deterministic to stochastic representation and back. (c) Experimental results of a Taylor bubble with dispersed bubbles in the wake by Kren et al. [97] (right panel).

5. Future challenges

The main aim of this paper is to summarize the current state of the art in the development of morphology-adaptive Eulerian methods and to initialize a homogenization process between the available methods. At this stage of development, there are many questions, challenges and problems, some of which will be discussed in this section, that remain open and must be dealt with. In this view, the paper aims at paving the way towards a collaborative effort and joint future research within the community to bring morphology-adaptive Eulerian methods into application and to establish sufficient confidence in their results. Extensive validation and benchmarking between simulation and experiment as well as between the various simulation frameworks listed in Section 3 based on the flow cases listed in Section 4 have to be a shared objective of the community. The test database needs to be extended towards heat and mass transfer, e.g., to look into nucleate boiling, the prediction of critical heat flux (CHF), or condensation processes in the pressurized thermal shock scenario in Fig. 2. Furthermore, the morphology-adaptive Eulerian methods have to prove their applicability and robustness in simulations at the industrial scale. The validation of the mechanism of transition between a stochastic and a deterministic representation or analogously between unresolved and resolved morphologies is a crucial task that has to be completed in order to establish a proper foundation of useful morphology-adaptive Eulerian methods. This includes studies on the accuracy of the results for partially-resolved morphologies as well as the breakup of resolved morphologies. Whereas the blended methods seem to behave reasonably well when agglomerating unresolved structures due to the presence of the interface compression, they seem to have some deficiencies when large interfaces break up into smaller ones. Furthermore, the interfacial drag modeling for resolved morphologies requires further investigation to give reasonable predictions for the velocity profiles and the turbulence near the interface. Separated methods seem to have a solution with the resolution-adaptive drag model by Meller et al. [36]. However, those methods have open questions as well, such as the development of robust and efficient transfers between the morphologies in case of varying mesh resolutions. Several of the models still miss a full coupling to a population balance model. Further flow morphologies, like thin-films need to be added to separated methods in the future. Another remaining challenge to all morphology-adaptive Eulerian methods is the turbulence modeling, in particular near the resolved interface. This gets particularly important if heat and mass transfer or phase change, e.g., due to condensation or evaporation, is of interest. All of this has to be addressed, at least partially, in order to tackle industrial cases.

CRediT authorship contribution statement

Fabian Schlegel: Writing – review & editing, Writing – original draft, Visualization, Validation, Supervision, Software, Project administration, Methodology, Investigation, Funding acquisition, Formal analysis, Conceptualization. **Amine Ben Hadj Ali:** Writing – review & editing, Writing – original draft, Software, Methodology. **Marco Colombo:** Writing – review & editing, Writing – original draft, Software, Methodology, Conceptualization. **Edo Frederix:** Writing – review & editing, Writing – original draft, Software, Methodology, Conceptualization. **Victor Habiyaremye:** Writing – review & editing, Writing – original draft, Software, Methodology, Conceptualization. **Susann Hänsch:** Writing – original draft, Software. **Thomas Höhne:** Writing – original draft, Software, Methodology. **Benjamin Krull:** Writing – review & editing, Writing – original draft, Supervision, Software, Methodology, Investigation, Conceptualization. **Ronald Lehnigk:** Writing – original draft, Supervision, Software, Methodology. **Dirk Lucas:** Supervision, Methodology, Funding acquisition, Conceptualization. **Richard Meller:** Writing – original draft, Software, Methodology, Conceptualization. **Mohit P. Tandon:** Writing – original draft, Software. **Michele Cristina Pedroso:** Software, Methodology, Conceptualization. **Juho Peltola:** Writing – review & editing, Software, Methodology, Conceptualization. **Matej Tekavčič:** Writing – review & editing, Writing – original draft, Software, Methodology, Conceptualization.

Declaration of competing interest

The authors declare that they have no known competing financial interests or personal relationships that could have appeared to influence the work reported in this paper.

Acknowledgments

The author from the Jožef Stefan Institute gratefully acknowledges the financial support provided by the Slovenian Research and Innovation Agency through the grant P2-0026. The author from the University of Sheffield acknowledges the support of the Engineering and Physical Sciences Research Council, United Kingdom through grants EP/S019871/1 and EP/S019871/2.

Data availability

Data will be made available on request.

References

[1] Soligo G, Roccon A, Soldati A. Turbulent flows with drops and bubbles: What numerical simulations can tell us—freeman scholar lecture. J Fluids Eng 2021;143(8):080801.
[2] Mirjalili S, Jain SS, Dodd M. Interface-capturing methods for two-phase flows: An overview and recent developments. Cent Turbul Res Annu Res Briefs 2017;2017(117–135):13.
[3] Elghobashi S. Direct numerical simulation of turbulent flows laden with droplets or bubbles. Annu Rev Fluid Mech 2019;51(1):217–44.
[4] Unverdi SO, Tryggvason G. A front-tracking method for viscous, incompressible, multi-fluid flows. J Comput Phys 1992;100(1):25–37. http://dx.doi.org/10.1016/0021-9991(92)90307-K, URL https://www.sciencedirect.com/science/article/pii/002199919290307K.
[5] Osher S, Fedkiw RP. Level set methods: An overview and some recent results. J Comput Phys 2001;169(2):463–502. http://dx.doi.org/10.1006/jcph.2000.6636, URL https://www.sciencedirect.com/science/article/pii/S0021999100966361.
[6] Jacqmin D. Calculation of two-phase navier–stokes flows using phase-field modeling. J Comput Phys 1999;155(1):96–127. http://dx.doi.org/10.1006/jcph.1999.6332, URL https://www.sciencedirect.com/science/article/pii/S0021999199963325.
[7] Roccon A, Zonta F, Soldati A. Phase-field modeling of complex interface dynamics in drop-laden turbulence. Phys Rev Fluids 2023;8:090501. http://dx.doi.org/10.1103/PhysRevFluids.8.090501, URL https://link.aps.org/doi/10.1103/PhysRevFluids.8.090501.
[8] Hirt C, Nichols B. Volume of fluid (vof) method for the dynamics of free boundaries. J Comput Phys 1981;39(1):201–25. http://dx.doi.org/10.1016/0021-9991(81)90145-5, URL https://www.sciencedirect.com/science/article/pii/0021999181901455.
[9] Scardovelli R, Zaleski S. Direct numerical simulation of free-surface and interfacial flow. Annu Rev Fluid Mech 1999;31(1):567–603.
[10] Ishii M, Hibiki T. Thermo-fluid dynamics of two-phase flow. Springer New York; 2011, http://dx.doi.org/10.1007/978-1-4419-7985-8.
[11] Zechner C, Nerli E, Norden C. Stochasticity and determinism in cell fate decisions. Development 2020;147(14):dev181495.
[12] Bestion D. System code models and capabilities. In: Vitanza C, editor. Thicket-2008. Pisa, Italy; 2008, p. 81–106.
[13] Drew DA, Passman SL. Theory of multicomponent fluids. Springer-Verlag New York; 1999, http://dx.doi.org/10.1007/b97678.
[14] Prosperetti A, Tryggvason G. Computational methods for multiphase flow. Cambridge University Press; 2009.
[15] Yeoh GH, Tu J, editors. Computational techniques for multiphase flows. Oxford: Butterworth-Heinemann; 2010, Includes bibliographical references (p. 607–626) and index. - Description based on print version record.
[16] Brackbill J, Kothe D, Zemach C. A continuum method for modeling surface tension. J Comput Phys 1992;100(2):335–54. http://dx.doi.org/10.1016/0021-9991(92)90240-y.
[17] Liovic P, Lakehal D. Subgrid-scale modelling of surface tension within interface tracking-based large eddy and interface simulation of 3d interfacial flows. Comput & Fluids 2012;63:27–46. http://dx.doi.org/10.1016/j.compfluid.2012.03.019, URL https://linkinghub.elsevier.com/retrieve/pii/S0045793012001168.
[18] Fleau S. Multifield approach and interface locating method for two-phase flows in nuclear power plant (Theses), Université Paris-Est; 2017, URL https://tel.archives-ouvertes.fr/tel-01621735.
[19] Mimouni S, Fleau S, Vincent S. CFD calculations of flow pattern maps and LES of multiphase flows. Nucl Eng Des 2018;321:118–31.
[20] Meller R, Schlegel F, Klein M. Sub-grid scale modelling and a-posteriori tests with a morphology adaptive multifield two-fluid model considering rising gas bubbles. Flow Turbul Combust 2022;108:895–922. http://dx.doi.org/10.1007/s10494-021-00293-8, URL https://link.springer.com/article/10.1007/s10494-021-00293-8.
[21] Ma T, Lucas D, Jakirlić S, Fröhlich J. Progress in the second-moment closure for bubbly flow based on direct numerical simulation data. J Fluid Mech 2020;883. http://dx.doi.org/10.1017/jfm.2019.851.
[22] Egorov Y. Validation of cfd codes with pts-relevant test cases. In: 5th EU-ROATOM framework programme. Technical report EVOL - ECORA - D 07, 2004, p. 1998–2002.
[23] Höhne T, Mehlhoop J-P. Validation of closure models for interfacial drag and turbulence in numerical simulations of horizontal stratified gas-liquid flows. Int J Multiph Flow 2014;62:1–16. http://dx.doi.org/10.1016/j.ijmultiphaseflow.2014.01.012, URL http://www.sciencedirect.com/science/article/pii/S0301932214000263.
[24] Porombka P, Höhne T. Drag and turbulence modelling for free surface flows within the two-fluid euler-euler framework. Chem Eng Sci 2015;134:348–59. http://dx.doi.org/10.1016/j.ces.2015.05.029.
[25] Gada VH, Tandon MP, Elias J, Vikulov R, Lo S. A large scale interface multi-fluid model for simulating multiphase flows. Appl Math Model 2017;44:189–204. http://dx.doi.org/10.1016/j.apm.2017.02.030.
[26] Frederix EMA, Mathur A, Dovizio D, Geurts BJ, Komen EMJ. Reynolds-averaged modeling of turbulence damping near a large-scale interface in two-phase flow. Nucl Eng Des 2018;333:122–30. http://dx.doi.org/10.1016/j.nucengdes.2018.04.010, URL https://linkinghub.elsevier.com/retrieve/pii/S0029549318304266.
[27] Dong Z, Bürgler M, Hohermuth B, Vetsch D. Density-based turbulence damping at large-scale interface for Reynolds-averaged two-fluid models. Chem Eng Sci 2022;247:116975. http://dx.doi.org/10.1016/j.ces.2021.116975.
[28] Tekavčič M, Meller R, Schlegel F. Validation of a morphology adaptive multifield two-fluid model considering counter-current stratified flow with interfacial turbulence damping. Nucl Eng Des 2021;379:111223. http://dx.doi.org/10.1016/j.nucengdes.2021.111223.
[29] Tandon M, Gada V, Ravi A. Adaptive interface sharpening scheme (adis) for modelling multiple flow regimes. In: 3rd International Conference on Numerical Methods in Multiphase Flows. 2017.
[30] Fan W, Anglart H. Varrhoturbvof: A new set of volume of fluid solvers for turbulent isothermal multiphase flows in openfoam. Comput Phys Comm 2020;247:106876. http://dx.doi.org/10.1016/j.cpc.2019.106876.
[31] Benz M, Schulenberg T. Validation analyses of advanced turbulence model approaches for stratified two-phase flows. WIT Trans Eng Sci 2015;89:361–72. http://dx.doi.org/10.2495/mpf150311.
[32] Benz M, Schulenberg T. Statistical modeling of stratified two-phase flow. J Nucl Eng Radiat Sci 2017;3(2). http://dx.doi.org/10.1115/1.4035564.
[33] Piña JS, Corzo S, Godino D, Ramajo D. Volume of fluid simulation of air–water co-current and counter-current flow with variable density turbulence formulation. Nucl Eng Des 2024;424:113217. http://dx.doi.org/10.1016/j.nucengdes.2024.113217.
[34] Pedroso MC, Weise J, Meller R, Schlegel F, de Cerqueira RFL, Paladino EE. Enhanced modeling for resolved morphologies in co-current stratified wavy pipe flows. Int J Multiph Flow 2025;192:105333. http://dx.doi.org/10.1016/j.ijmultiphaseflow.2025.105333, URL https://www.sciencedirect.com/science/article/pii/S0301932225002113.
[35] Höhne T, Hänsch S. A droplet entrainment model for horizontal segregated flows. Nucl Eng Des 2015;286:18–26. http://dx.doi.org/10.1016/j.nucengdes.2015.01.013, URL http://linkinghub.elsevier.com/retrieve/pii/S0029549315000540.
[36] Meller R, Tekavčič M, Krull B, Schlegel F. Momentum exchange modeling for coarsely resolved interfaces in a multifield two-fluid model. Internat J Numer Methods Fluids 2023;95(9):1521–45. http://dx.doi.org/10.1002/fld.5215, URL https://onlinelibrary.wiley.com/doi/full/10.1002/fld.5215.
[37] Krull B, Meller R, Tekavčič M, Schlegel F. A filtering approach for applying the two-fluid model to gas-liquid flows on high resolution grids. Chem Eng Sci 2024;290:119909. http://dx.doi.org/10.1016/j.ces.2024.119909.
[38] Schlegel F, Hänsch S, Krull B, Meller R, Kota SP. Comparison of upper boundary treatments for bubble column simulations with the two-fluid model. Exp Comput Multiph Flow 2025;7:227–44. http://dx.doi.org/10.1007/s42757-025-0241-6.
[39] Meller R, Schlegel F, Lucas D. Basic verification of a numerical framework applied to a morphology adaptive multifield two-fluid model considering bubble motions. Internat J Numer Methods Fluids 2021;93(3):748–73. http://dx.doi.org/10.1002/fld.4907.
[40] De Santis A, Colombo M, Hanson B, Fairweather M. A generalized multiphase modelling approach for multiscale flows. J Comput Phys 2021;436:110321. http://dx.doi.org/10.1016/j.jcp.2021.110321.
[41] Colombo M, De Santis A, Hanson B, Fairweather M. Prediction of horizontal gas-liquid segregated flow regimes with an all flow regime multifluid model. Processes 2022;10(5):920. http://dx.doi.org/10.3390/pr10050920.
[42] Weller HG. A new approach to vof-based interface capturing methods for incompressible and compressible flow. Technical report, 9 Albert Road, Caversham, Reading RG4 7AN, United Kingdom: OpenCFD Ltd.; 2008.
[43] Colombo M, Vivaldi D, Baccou J. Prediction of the flow patterns in a steam generator tube bundle configuration with all-flow-regime CFD models. In: 20th international topical meeting on nuclear reactor thermal hydraulics. NURETH-20, 2023.

[44] Aburema H, Hanson B, Fairweather M, Colombo M. A generalised multiphase modelling approach with heat transfer and thermal phase change. Int J Heat Fluid Flow 2024;109:109524. http://dx.doi.org/10.1016/j.ijheatfluidflow.2024.109524, URL https://www.sciencedirect.com/science/article/pii/S0142727X24002492.

[45] Colombo M, Fairweather M. Prediction of bubbly flow and flow regime development in a horizontal air–water pipe flow with a morphology-adaptive multifluid CFD model. Int J Multiph Flow 2025;184:105112. http://dx.doi.org/10.1016/j.ijmultiphaseflow.2024.105112, URL https://www.sciencedirect.com/science/article/pii/S0301932224003884.

[46] Hänsch S, Lucas D, Krepper E, Höhne T. A multi-field two-fluid concept for transitions between different scales of interfacial structures. Int J Multiph Flow 2012;47:171–82.

[47] Hänsch S, Lucas D, Höhne T, Krepper E. Application of a new concept for multi-scale interfacial structures to the dam-break case with an obstacle. Nucl Eng Des 2014;279:171–81. http://dx.doi.org/10.1016/j.nucengdes.2014.02.006, URL https://linkinghub.elsevier.com/retrieve/pii/S0029549314000880.

[48] Montoya G, Baglietto E, Lucas D, Krepper E, Höhne T. Comparative analysis of high void fraction regimes using an averaging euler-euler multi-fluid approach and a generalized two-phase flow (gentop) concept. In: 22st international conference on nuclear engineering. ICONE22, 2014.

[49] Montoya G, Baglietto E, Lucas D. Implementation and validation of a surface tension model for the multi-scale approach gentop. In: 16th international topical meeting on nuclear reactor thermal hydraulics. NURETH-16, vol. 16, 2015, p. 4219–32.

[50] Höhne T, Krepper E, Montoya G, Lucas D. CFD-simulation of boiling in a heated pipe including flow pattern transitions using the GENTOP concept. Nucl Eng Des 2017;322:165–76. http://dx.doi.org/10.1016/j.nucengdes.2017.06.047, URL https://linkinghub.elsevier.com/retrieve/pii/S0029549317303199.

[51] Setoodeh H, Shabestary AM, Ding W, Lucas D, Hampel U. CFD-modelling of boiling in a heated pipe including flow pattern transition. Appl Therm Eng 2022;204:117962. http://dx.doi.org/10.1016/j.applthermaleng.2021.117962.

[52] Mathur A, Dovizio D, Frederix EMA, Komen EMJ. A hybrid dispersed-large interface solver for multi-scale two-phase flow modelling. Nucl Eng Des 2019;344:69–82. http://dx.doi.org/10.1016/j.nucengdes.2019.01.020, URL https://linkinghub.elsevier.com/retrieve/pii/S0029549318309920.

[53] Frederix EMA, Dovizio D, Mathur A, Komen EMJ. All-regime two-phase flow modeling using a novel four-field large interface simulation approach. Int J Multiph Flow 2021;145:103822. http://dx.doi.org/10.1016/j.ijmultiphaseflow.2021.103822.

[54] Frederix E, Cox T, Kuerten J, Komen E. Poly-dispersed modeling of bubbly flow using the log-normal size distribution. Chem Eng Sci 2019;201:237–46. http://dx.doi.org/10.1016/j.ces.2019.02.013, URL https://www.sciencedirect.com/science/article/pii/S0009250919301757.

[55] Habiyaremye V, Komen E, Kuerten J, Frederix E. Modeling of bubble coalescence and break-up using the log-normal method of moments. Chem Eng Sci 2022;253:117577. http://dx.doi.org/10.1016/j.ces.2022.117577, URL https://www.sciencedirect.com/science/article/pii/S0009250922001610.

[56] Schlegel F, Meller R, Krull B, Lehnigk R, Tekavčič M. OpenFOAM-Hybrid: A morphology adaptive multifield two-fluid model. Nucl Sci Eng 2023;197(10):2620–33. http://dx.doi.org/10.1080/00295639.2022.2120316, Selected papers from the 19th International Topical Meeting on Nuclear Reactor Thermal Hydraulics (NURETH-19).

[57] Hänsch S, Evdokimov I, Schlegel F, Lucas D. A workflow for the sustainable development of closure models for bubbly flows. Chem Eng Sci 2021;244:116807. http://dx.doi.org/10.1016/j.ces.2021.116807.

[58] Štrubelj L, Tiselj I. Two-fluid model with interface sharpening. Internat J Numer Methods Engrg 2011;85:575–90. http://dx.doi.org/10.1002/nme.2978.

[59] Krull B, Meller R, Schlegel F, Tekavčič M. Adaptive modelling of bubbly flows: from unresolved to resolved representation. In: 5th international conference on numerical methods in multiphase flows. Reykjavik, Iceland; 2024.

[60] Meller R, Krull B, Schlegel F, Tekavčič M. Numerical transfer towards unresolved morphology representation in the MultiMorph model. Nucl Eng Des 2024;428:113470. http://dx.doi.org/10.1016/j.nucengdes.2024.113470, URL https://www.sciencedirect.com/science/article/pii/S0029549324005703.

[61] Schlegel F, Bilde KG, Draw M, Evdokimov I, Hänsch S, Kamble VV, Khan H, Krull B, Lehnigk R, Li J, Lyu H, Meller R, Petelin G, Kota SP, Tekavčič M. Multiphase code repository by HZDR for openFOAM foundation software (version 12-s.1-hzdr.1). RODARE; 2024, URL https://rodare.hzdr.de/record/767.

[62] Zhang T, Huang G, Yin J, Zhang Z, Wang D, Sun Y, Liao Y. Investigation on swirl instability in a vane-type separator with tomographic particle image velocimetry. J Fluids Eng 2022;144(5). http://dx.doi.org/10.1115/1.4052547.

[63] Yin J, Zhang T, Krull B, Meller R, Schlegel F, Lucas D, Wang D, Liao Y. A CFD approach for the flow regime transition in a vane-type gas-liquid separator. Int J Multiph Flow 2023;159:104320. http://dx.doi.org/10.1016/j.ijmultiphaseflow.2022.104320.

[64] Wang L-S, Krull B, Lucas D, Meller R, Schlegel F, Tekavčič M, Xu J-Y. Simulation of droplet entrainment in annular flow with a morphology adaptive multi-field two-fluid model. Phys Fluids 2023;35(10). http://dx.doi.org/10.1063/5.0169288.

[65] Wiedemann P, Meller R, Schubert M, Hampel U. Application of a hybrid multiphase CFD approach to the simulation of gas–liquid flow at a trapezoid fixed valve for distillation trays. Chem Eng Res Des 2023;193:777–86. http://dx.doi.org/10.1016/j.cherd.2023.04.016.

[66] Krull B, Bilde K, Kringel C, Meller R, Molbak V, Papaioannou G, Schlegel F, Tekavčič M, Tziaros F. Numerical modelling of air-induced drag reduction allowing the transition between bubbly, air layer and mixed regimes. Appl Ocean Res 2026;166:104892.

[67] Höhne T, Porombka P, Sáez S Moya. Validation of aiad sub-models for advanced numerical modelling of horizontal two-phase flows. Fluids 2020;5(3). http://dx.doi.org/10.3390/fluids5030102, URL https://www.mdpi.com/2311-5521/5/3/102.

[68] Gada VH, Eliasm. A large scale interface multifluid model for simulating multiphase flows. In: Solnordal CB, Liovic, editors. 11th international conference on CFD in the minerals and process industries. 2015, URL http://www.cfd.com.au/cfd_conf15/PDFs/079GAD.pdf.

[69] Gada V, Tandon M, Ravi A. Large interface detection method for multiple flow regime multiphase model. In: 7th international fluid mechanics and fluid power conference. 2018.

[70] Coste P. A large interface model for two-phase CFD. Nucl Eng Des 2013;255:38–50. http://dx.doi.org/10.1016/j.nucengdes.2012.10.008, URL http://www.sciencedirect.com/science/article/pii/S0029549312005213.

[71] Gada V, Tandon M. A wall-function type interface turbulence damping method for multiple flow regimes with large scale interfaces. In: 21st international topical meeting on nuclear reactor thermal hydraulics. 2025.

[72] Rider WJ, Kothe DB. Reconstructing volume tracking. J Comput Phys 1998;141(2):112–52. http://dx.doi.org/10.1006/jcph.1998.5906, URL http://www.sciencedirect.com/science/article/pii/S002199919895906X.

[73] Coste P, Laviéville J. A turbulence model for large interfaces in high Reynolds two-phase CFD. Nucl Eng Des 2015;284:162–75. http://dx.doi.org/10.1016/j.nucengdes.2014.12.004.

[74] Gada V, Tandon M. Size distribution modelling for multiple flow regimes with large scale interfaces. In: 12th international conference of multiphase flows. 2025.

[75] Tandon M, Khanolkar A, Splawski A, Lo S. Validation of numerical simulations of gas-liquid systems in a vertical pipe. In: 8th international conference of multiphase flows. 2013.

[76] Brocchini M, Peregrine D. The dynamics of strong turbulence at free surfaces part 1. description. J Fluid Mech 2001;449:225–54. http://dx.doi.org/10.1017/S0022112001006012.

[77] Yu X, Hendrickson K, Yue DKP. Scale separation and dependence of entrainment bubble-size distribution in free-surface turbulence. J Fluid Mech 2020;885:R2. http://dx.doi.org/10.1017/jfm.2019.986.

[78] Marschall H. Towards the numerical simulation of multi-scale two-phase flows (Ph.D. thesis), Technische Universität Muenchen, Lehrstuhl I für Technische Chemie; 2011.

[79] Fabre J, Masbernat L, Suzanne C. Experimental data set no. 7: Stratified flow, part i: Local structure. Multiph Sci Technol 1987;3(1–4):285–301. http://dx.doi.org/10.1615/MultScienTechn.v3.i1-4.120.

[80] Coste P, Laviéville J, Pouvreau J, Baudry C, Guingo M, Douce A. Validation of the large interface method of NEPTUNE CFD 1.0.8 for pressurizedthermal shock (PTS) applications. Nucl Eng Des 2012;253:296–310. http://dx.doi.org/10.1016/j.nucengdes.2011.08.066, URL http://www.sciencedirect.com/science/article/pii/S0029549311006911.

[81] Colombo M, De Santis A, Hanson B, Fairweather M. A Generalized Multifluid Modelling Approach (GEMMA): application to multiple flow regime phenomena in nuclear reactor thermal hydraulics. In: Proceedings of NURETH-19. 2022.

[82] Stäbler T. Experimentelle Untersuchung und physikalische beschreibung der schichtenströmung in horizontalen kanälen (Ph.D. thesis), University of Stuttgart; 2007.

[83] Yan H, Zhang H, Höhne T, Liao Y, Lucas D, Liu L. Numerical modeling of horizontal stratified two-phase flows using the aiad model. Front Energy Res 10:2022. http://dx.doi.org/10.3389/fenrg.2022.939499, URL https://www.frontiersin.org/journals/energy-research/articles/10.3389/fenrg.2022.939499.

[84] Štrubelj L, Tiselj I. Numerical simulations of basic interfacial instabilities with incompressible two-fluid model. Nucl Eng Des 2011;241(4):1018–23. http://dx.doi.org/10.1016/j.nucengdes.2010.03.032.

[85] Thorpe SA. Experiments on the instability of stratified shear flows: immiscible fluids. J Fluid Mech 1969;39(1):25–48. http://dx.doi.org/10.1017/s0022112069002023.

[86] Vallée C, Lucas D, Beyer M, Pietruske H, Schütz P, Carl H. Experimental CFD grade data for stratified two-phase flows. Nucl Eng Des 2010;240(9):2347–56. http://dx.doi.org/10.1016/j.nucengdes.2009.11.011.

[87] Lim IS, Tankin RS, Yuen MC. Condensation measurement of horizontal cocurrent steam/water flow. J Heat Transf 1984;106(2):425–32. http://dx.doi.org/10.1115/1.3246689.

[88] Friedemann C, Mortensen M, Nossen J. Gas–liquid slug flow in a horizontal concentric annulus, a comparison of numerical simulations and experimental data. Int J Heat Fluid Flow 2019;78:108437. http://dx.doi.org/10.1016/j.ijheatfluidflow.2019.108437.

[89] Hysing S, Turek S, Kuzmin D, Parolini N, Burman E, Ganesan S, Tobiska L. Quantitative benchmark computations of two-dimensional bubble dynamics. Internat J Numer Methods Fluids 2009;60(11):1259–88. http://dx.doi.org/10.1002/fld.1934.

[90] Adelsberger J, Esser P, Griebel M, Groß S, Klitz M, Rüttgers A. 3D incompressible two-phase flow benchmark computations for rising droplets. In: 11th world congress on computational mechanics. WCCM XI, vol. 179, Barcelona, Spain; 2014, URL https://www.researchgate.net/publication/287994803_3D_incompressible_two-phase_flow_benchmark_computations_for_rising_droplets.

[91] Bhaga D, Weber ME. Bubbles in viscous liquids: shapes, wakes and velocities. J Fluid Mech 1981;105:61–85. http://dx.doi.org/10.1017/s002211208100311x.

[92] Balcazar N, Lehmkuhl O, Jofre L, Oliva A. Level-set simulations of buoyancy-driven motion of single and multiple bubbles. Int J Heat Fluid Flow 2015;56:91–107.

[93] Sharaf DM, Premlata AR, Tripathi MK, Karri B, Sahu KC. Shapes and paths of an air bubble rising in quiescent liquids. Phys Fluids 2017;29(12):122104. http://dx.doi.org/10.1063/1.5006726.

[94] Yan K, Che D. A coupled model for simulation of the gas-liquid two-phase flow with complex flow patterns. Int J Multiph Flow 2010;36:333.

[95] Mikuž B, Kamnikar J, Prošek J, Tiselj I. Experimental observation of taylor bubble disintegration in turbulent flow. In: Proceedings of the international conference nuclear energy for New Europe, Portorož, Slovenia. vol. 12, 2019, p. 0–38.

[96] Mikuž B, Frederix E, Komen E, Tiselj I. Taylor bubble behaviour in turbulent flow regime. In: Computational fluid dynamics for nuclear reactor safety. CFD4NRS-8, vol. 12, 2020.

[97] Kren J, Zajec B, Tiselj I, Shawish SE, Perne Ž, Tekavčič M, Mikuž B. Dynamics of taylor bubble interface in vertical turbulent counter-current flow. Int J Multiph Flow 2023;165:104482. http://dx.doi.org/10.1016/j.ijmultiphaseflow.2023.104482.

[98] Tiselj I, Kren J, Mikuž B, Nop R, Burlot A, Hamrit G. Experimental and numerical study of taylor bubble in counter-current turbulent flow. Arab J Sci Eng 2024. http://dx.doi.org/10.1007/s13369-024-09489-2.

[99] Kren J, Tiselj I, Mikuž B. Experimental observation of taylor bubble disintegration in turbulent flow. In: International conference nuclear energy for new europe. NENE2024, 2024, p. 303.1–8, URL https://www.djs.si/nene2024proceedings/pdf/NENE2024_303.pdf.

[100] Frederix EMA, Komen EMJ, Tiselj I, Mikuž B. Les of turbulent co-current taylor bubble flow. Flow Turbul Combust 2020;105(2):471–95. http://dx.doi.org/10.1007/s10494-020-00118-0.

[101] Kren J, Frederix EMA, Tiselj I, Mikuž B. Numerical study of taylor bubble breakup in counter-current flow using large eddy simulation. Phys Fluids 2024;36(2). http://dx.doi.org/10.1063/5.0186236.

[102] Santarelli C, Fröhlich J. Direct numerical simulations of spherical bubbles in vertical turbulent channel flow. influence of bubble size and bidispersity. Int J Multiph Flow 2016;81:27–45. http://dx.doi.org/10.1016/j.ijmultiphaseflow.2016.01.004, URL https://www.sciencedirect.com/science/article/pii/S0301932216000045.

[103] Iguchi M, Okita K, Yamamoto F. Mean velocity and turbulence characteristics of water flow in the bubble dispersion region induced by plunging water jet. Int J Multiph Flow 1998;24:523–37.

[104] Bonetto F, Lahey R. An experimental study on air carryunder due to a plunging liquid jet. Int J Multiph Flow 1993;19(2):281–94.

[105] Chanson H, Aoki S, Hoque A. Physical modelling and similitude of air bubble entrainment at vertical circular plunging jets. Chem Eng Sci 2004;59:747–54. http://dx.doi.org/10.1016/j.ces.2003.11.016.

[106] Qu XL, Khezzar L, Danciu D, Labois M, Lakehal D. Characterization of plunging liquid jets: A combined experimental and numerical investigation. Int J Multiph Flow 2011;37:722–31.

[107] Danciu D-V, Kendil FZ, Mishra A, Schmidtke M, Lucas D, Hampel U. Velocity fields under impinging jets with gas entrainment. In: 7th international conference on multiphase flow. 2010.

[108] Meller R, Krull B, Schlegel F, Tekavčič M. Numerical transfer towards unresolved morphology representation in the multimorph model. In: Bajorek SM, editor. Proceedings of the 20th internationalTopical meeting on nuclear reactorThermal hydraulics. NURETH-20, vol. 60515, Downers Grove, Illinois: American Nuclear Society, Incorporated; 2023, p. 693–706, URL https://www.ans.org/pubs/proceedings/article-54124/.

[109] Shonibare OY, Wardle KE. Numerical investigation of vertical plunging jet using a hybrid multifluid-VOF multiphase CFD solver. Int J Chem Eng 2015;2015:1–14.

[110] Bottin M, Berlandis J, Hervieu E, Lance M, Marchand M, Öztürk O, Serre G. Experimental investigation of a developing two-phase bubbly flow in horizontal pipe. Int J Multiph Flow 2014;60:161–79. http://dx.doi.org/10.1016/j.ijmultiphaseflow.2013.12.010.

[111] Weise J, de Cerqueira RFL, Paladino EE. Experimental study of the transient gas-liquid flow through an orifice plate using high speed camera and differential pressure measurement. In: Proceedings of the 19th Brazilian congress of thermal sciences and engineering, Bento Goncalves, Brazil. 2022.

[112] Porombka P, Boden S, Lucas D, Hampel U. Horizontal annular flow through orifice studied by x-ray microtomography. Exp Fluids 2021;62(1). http://dx.doi.org/10.1007/s00348-020-03091-6.

[113] Gabriel SG. Experimentelle untersuchung der tropfenabscheidung einer horizontalen, entgegengerichteten wasser/luft-schichtenströmung (Ph.D. thesis), Universität Stuttgart; 2014, KIT Scientific Reports ; 7683.

[114] Höhne T, Gabriel S. Simulation of a counter-current horizontal gas-liquid flow experiment at the wenka channel using a droplet entrainment model. Ann Nucl Energy 2018;121:414–25. http://dx.doi.org/10.1016/j.anucene.2018.07.047.

[115] Lucas D, Beyer M, Szalinski L, Schuetz P. A new database on the evolution of air–water flows along a large vertical pipe. Int J Therm Sci 2010;49:664–74. http://dx.doi.org/10.1016/j.ijthermalsci.2009.11.008.

[116] Černe G, Petelin S, Tiselj I. Coupling of the interface tracking and the two-fluid models for the simulation of incompressible two-phase flow. J Comput Phys 2001;171:776.

[117] Canot E, Vincent S. Test-case no 4: Rayleigh-taylor instability for isothermal, incompressible and non-viscous fluids (pa). Multiph Sci Technol 2004;16(1–3):23–9. http://dx.doi.org/10.1615/multscientechn.v16.i1-3.50.

[118] Štrubelj L. Numerical simulations of stratified two-phase flows with two-fluid model and interface sharpening (Ph.D. thesis), University of Ljubljana, Faculty of Mathematics and Physics, Department of Physics; 2009.

[119] Rezende R, Almeida R, d. Souza AU, Souza S. A two-fluid model with a tensor closure model approach for free surface flow simulations. Chem Eng Sci 2015;122:596–613. http://dx.doi.org/10.1016/j.ces.2014.07.064.